J. Phys. B: At. Mol. Opt. Phys. **30** (1997) 3031–3048. Printed in the UK PII: S0953-4075(97)80403-8

On the low-energy rotationally inelastic collisions of H^- with H_2 molecules

Franco A Gianturco† and Sanjay Kumar

Dipartimento di Chimica, Università di Roma, 'La Sapienza', Città Universitaria, 00185 Rome, Italy

Received 19 December 1996, in final form 12 May 1997

Abstract. The rotationally inelastic cross sections, integral and differential, are computed as quantum processes using a published interaction potential and are compared with recently available experimental data at low collision energies. Different coupling approximations are analysed and the mainly repulsive interaction potential is confronted with the one exhibited by the $H + H_2$ system. It is found that a full coupling of angular momenta is needed for accurate comparisons and that the long-range anisotropy of the employed intraction is still not adequate to quantitatively reproduce the experimental data.

1. Introduction

Both H^+ and H^- constitute the simplest possible positive and negative ions and their dynamical interactions with molecular targets, especially with the smaller and most common diatomic molecules, is clearly of fundamental importance for the study of ion–molecule processes. Despite the great strides made recently both in theory and experiments, however (see, for example Niedner-Schatterburg and Toennies 1992, Gianturco and Kumar 1995a), the interaction forces acting during their low-energy dynamics are not fully understood yet and are only now beginning to be unravelled for the processes involving the negative ions (Müller *et al* 1996, Zimmer and Linder 1992, Hege and Linder 1985, Stärck and Meyer 1993, Gianturco and Kumar 1995b, c, Gianturco *et al* 1996, Mahapatra *et al* 1995, Mahapatra and Sathyamurty 1996).

In contrast to the 'structureless' positive ion, in fact, the H^- projectile possesses a rather delicate structure with respect to the detachment process: $H^- \rightarrow H + e^-$, in which correlation forces play a rather important role. Collisional processes can therefore destroy such a structure rather easily, giving rise to electron detachment and resonant charge transfer collisions that become dominant with respect to the rearrangement and inelastic channels even at fairly low collision energies (Reinig *et al* 1992). On the other hand, crossed molecular beam experiments which involved grazing collisions in the forward scattering ($\theta \leqslant 1.0^\circ$), at energies which varied between 20 and ≈ 200 eV (Hege *et al* 1985), provided us with an appreciable chance for the survival of H^- during the scattering process. In such arrangements the experiments showed an interesting and intriguing selectivity for vibrational inelasticity when compared with the data of similar processes with protons as projectiles. To explain such selectivity, the authors proposed a 'transient change transfer' mechanism whereby the diffuse electronic charge distribution of the incoming H^- flows over the target

† Author to whom correspondence should be sent. E-mail address: FAGIANT@CASPUR.IT

0953-4075/97/133031+18$19.50

molecule and occupies, when available, one of its antibonding molecular orbitals (MOs). This 'transient' excitation results in a change of the stretching force constant and therefore of the vibrational excitation probabilities. Further theoretical studies on the structure and dynamics of $H_2 - H^-$ and $N_2 - H^-$ (Gianturco and Kumar 1995a–c, Gianturco *et al* 1996) have shown that the relative lifetimes of $H_2^-(\approx 10^{-16}$ s) and $N_2^-(\approx 10^{-14}$ s) indeed play a crucial role for the interpretation of the experimental findings.

It therefore becomes of interest to further probe other aspects of both the interaction forces and the dynamical outcomes for the simpler molecular targets in collision with H^-. To this end, the recent experimental data of Müller *et al* (1996) provide specific indications on the rotationally inelastic efficiency of $H^- - H_2$ collisions and on the general behaviour of the excitation processes at low energy. The present study is therefore directed at analysing rotational inelasticity in $H^- - H_2$ scattering and hopes to establish the relative reliability of using various possible quantum treatments of the collision processes. In the event, we will also analyse the quality of the currently available computed potential energy surface (PES) (Stärck and Meyer 1993) when used to describe rotational excitation processes.

The paper is organized as follows. Section 2 analyses the available PES and compares it with that of the similar but neutral system, $H + H_2$. Section 3 describes the different coupling approximations used in the present quantum scattering calculations and compares them with our exact close-coupling calculations. Section 4 makes a detailed comparison with the available experiments. Finally, in section 5 our conclusions are summarized.

2. A comparison with the $H + H_2$ interaction

As mentioned in the introduction, the $H^- + H_2$ system has a number of interesting features related to the occurrence of the electron detachment channel reaction

$$H^- + H_2 \rightarrow H_2 + H + e^- \tag{1}$$

that has a detachment threshold of about 1.45 eV (Zimmer and Linder 1992), and a further rearrangement channel

$$H^- + D_2 \rightarrow HD + D^- \tag{2}$$

with an energy threshold of about 0.42 eV (Zimmer and Linder 1992). Thus, the study of negative ion reactions has opened up an interesting avenue for the analysis of a novel class of ion–molecule processes (Metz *et al* 1992). A recent series of studies of collinear inelastic and reactive processes involving H^- on H_2 (Mahapatra *et al* 1995, Mahapatra and Sathyamurty 1996) has pointed out the presence of a large number of resonances in both channels and also discussed the similarity of the ionic interaction with the corresponding neutral analogue:

$$H + H_2 \rightarrow H_2 + H \tag{3}$$

undergoing the same rearrangement process as in (2). It is in fact, interesting to note that the linear transition state (TS) configuration for H_3^- occurs for $r_{H-H^-} = r_{H-H} = 1.997\ a_0$ and with a barrier height of 0.4684 eV (Stärck and Meyer 1993), while the corresponding TS configuration for its neutral analogue takes place with an r_{H-H} value of $1.757\ a_0$ and a barrier height of 0.4249 eV (Truhlar and Herowitz 1978). Furthermore, the analysis of the general behaviour of the lowest PES for H_3^- (see, for example Gianturco and Kumar 1996) shows that the multipolar coefficients of the usual expansion of the full PES

$$V^{H_3^-}(R, r, \gamma) = \sum_\lambda V_\lambda^{H_3^-}(R, r) P_\lambda(\cos\gamma) \tag{4}$$

where R is the collision coordinate, r is the molecular bond distance and $\gamma = \arccos \hat{R}\hat{r}$, remains largely repulsive in the short and intermediate ranges of R values and for most orientations, while only a very shallow attractive well occurs for the $\lambda = 2$ coefficient, at about 2.5 a_0, and indicates a preference for collinear configurations as found for the TS geometry. All the higher terms therefore remain repulsive and rather short ranged in character.

This behaviour is indeed similar to the one shown by the $H + H_2$ system along its subreactive PES, as discussed in several papers on the rotational excitation of the H_3 system (Choi and Tang 1975, Sun and Dalgarno 1994, Boothroyd *et al* 1996) and therefore it becomes useful for the present study to analyse this qualitative similarity further in terms of PES shapes. For this aspect of the problem, one should also see the recent work of Flower and Wroe (1996) on rate constants from integral state-to-state cross sections.

The results presented in figure 1 indicate in more detail the behaviour of the multiple coefficients of equation (4) for both systems. The results for the $H^- - H_2$ system, with H_2 treated as a rigid rotor (RR) at its equilibrium geometry, are shown on the right-hand side of the figure and they are those of the PES of Stärck and Meyer (1993) as discussed in our earlier work (Gianturco and Kumar 1995a–c, 1996). On the other hand, the results for the $H + H_2$ system are presented on the left-hand side of the same figure and are taken from the recent calculations of Boothroyd *et al* (1996). One can clearly make the following comments on the behaviour exhibited by both sets of multipolar coefficients.

(i) The spherical coefficient, V_0 is clearly mostly repulsive for both systems and the onset of its repulsive wall occurs further outside of all the higher coefficients. The insets clearly show that they also exhibit very shallow wells for R values beyond about 6 a_0. However, the H^- projectile causes, as expected, a much stronger attractive well than the neutral counterpart.

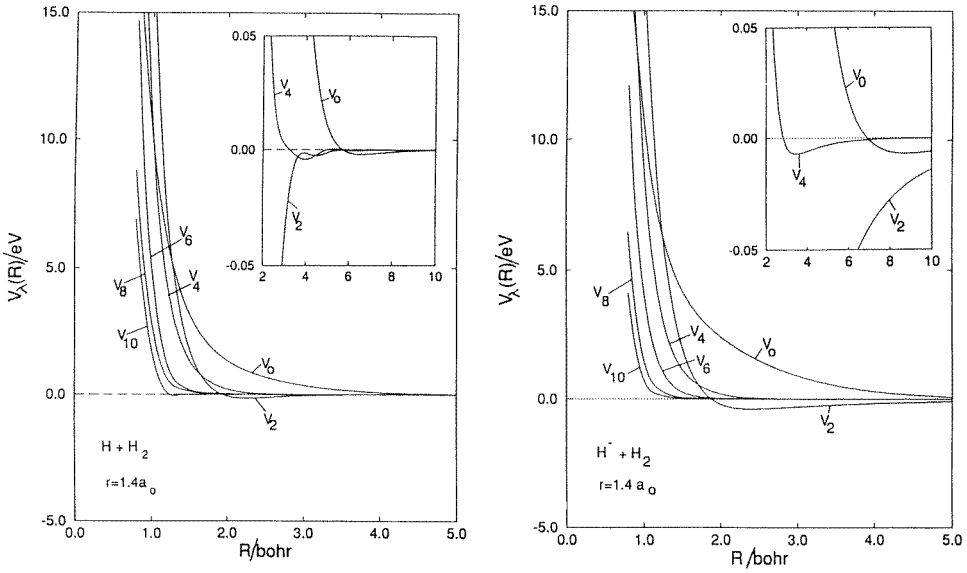

Figure 1. Computed potential energy surface multipolar coefficients for the $H+H_2$ system (left) and $H^- + H_2$ system (right) in the case of rigid rotor targets. The insets show the behaviour of the lower coefficents on an enlarged scale. The left PES is from Bothroyd *et al* (1996), while the right PES is from Stärck and Meyer (1993).

(ii) All the higher, more anisotropic coefficients are invariably repulsive in both systems, for $\lambda > 4$, and are also important at increasingly shorter distances of the projectile from the system centre of mass. Obviously, only an increasingly deeper penetration of H or of H^- into the molecular region can let them probe the stronger anisotropy of the interaction.

(iii) In the case of H_3, only the V_2 and V_4 contributions show attractive wells and indicate the $\lambda = 2$ term as being by far the strongest. They both become, at large R values, markedly more repulsive than any of the coefficients with higher λ. Very similarly, the H^- projectile shows that its two coefficents with the same λ, V_2 and V_4, are indeed attractive in the outer region and become repulsive at very similar R values which are external to the higher-λ coefficients. As expected, the H^- partner produces a stronger interaction in the long-range region because of the stronger polarization and electrostatic effects from the ionic projectile. Furthermore, the weakly bound H^- projectile causes strong dispersion interaction with the neutral molecule and therefore induces additional attractive effects in the long-range region.

In conclusion, we see from figure 1 that the anisotropy in the short-range region is very similar in both systems, while the long-range intraction is stronger with the H^- partner and extends over a larger range of R values. It is this difference which we expect to affect rather visibly affect the behaviour of low-energy rotational excitation collisions.

2.1. Rotationally inelastic angular distributions

In order to further analyse the similarities, and the expected differences, between the two short-range interactions briefly described above we find it instructive to compare the behaviours of their rotationally inelastic partial differential cross sections. The calculations were carried out using a rigorous close-coupling (CC) treatment of the relevant angular momenta, the details of our computational procedure will be discussed in more detail in the following section. Suffice it to say here that all the tests for multichannel convergence of the results were met by the present data and the employed PESs were the one by Stärck and Meyer (1993) for the $H^- - H_2$ system and the one quoted by Boothroyd *et al* (1996) for the $H + H_2$ system.

In figure 2 we report two types of rotationally inelastic processes: the $(j = 0) \rightarrow (j' = 2)$ transition for the para-H_2 targets and the $(j = 0) \rightarrow (j' = 4)$ transition for the same targets. Both excitation processes are, in fact, of interest here because each direct dynamical transition is linked to the strength and range of action of a specific multipolar term in equation (4), so that we can qualitatively say that the $\Delta j = 2$ excitation relates, to first order, to the $\lambda = 2$ term while the $\Delta j = 4$ transition is most directly coupled to the $\lambda = 4$ term of the anisotropic potential. Finally, we represent the inelastic transitions for the neutral analogue by the broken curves, while the corresponding transitions for the ionic system are given by the full curves.

We have also decided to span a rather broad range of translational energies which go from 0.1 eV above threshold up to 0.5 eV. From the shape of the interactions in figure 1 we see that such energies are well within the range of impact parameters where the classical turning points are definitely sampling the lower coefficients at most angles, thereby making the direct processes under study those most likely to occur. The following considerations can be made by a perusal of the results displayed in figure 2.

(i) The inelastic efficiency of the ionic system is, as expected, markedly larger than that of its neutral counterpart. The present differential, inelastic cross sections are, in fact, much larger for $H^- + H_2$ at nearly all angles and at all energies. Only the $\Delta j = 2$ transitions appear to be slightly larger for the $H + H_2$ in the back-scattering region.

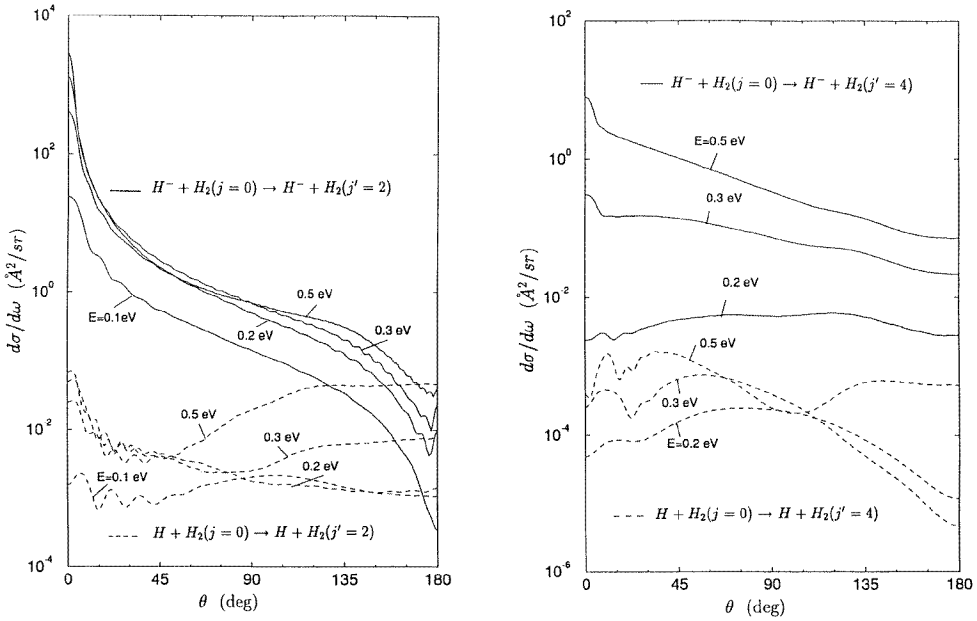

Figure 2. Computed close-coupling differential cross sections, at various collision energies for the rotational excitations ($j = 0 \rightarrow j' = 2$), on the left-hand side, and ($j = 0 \rightarrow j' = 4$) on the right-hand side. Full curves: $H^- - H_2$; broken curves $H + H_2$.

(ii) The negative ion projectile also exhibits a very marked forward scattering behaviour, in the case of the $\Delta j = 2$ excitation process, with respect to that of the neutral system. The dominance of the $V_2(R)$ coefficient of equation (4) during the dynamical coupling also indicates that its long-range part is much stronger in the latter case than in the former, due to the dual presence of strong dipole polarizability coefficient and of electrostatic quadrupole interaction as leading terms of the perturbation expansion (Stärck and Meyer 1993). Hence the effect is found in the final, inelastic angular distribution of figure 2.

(iii) The short-range nature of the neutral interaction allows here a clearer presence of fast oscillations in the small-angle distribution because of the relatively smaller number of partial waves which contribute to the scattering event (Gianturco 1979). On the other hand, the long-range additional contributions for the ionic system cause marked quenching of such oscillations, as reported by the present calculations, since a large number of partial waves is contributing to the scattering process also in the small angle region.

In view of summing up the above findings, we can say that although the $H^- - H_2$ interaction appears at first to be qualitatively similar to its neutral counterpart, the existing physical differences due to the long-range ionic interaction in the former system are seen to affect rather markedly the dynamical outcomes of the inelastic scattering processes. We therefore expect, as already seen in the collinear processes (Mahapatra *et al* 1995), that the inelastic cross sections might show, through other aspects of their behaviour, the effects from such differences in the long-range interaction.

3. A comparison of coupling dynamics

Because of the special nature of the interaction potential between the negative ion and the H_2 target, we need to analyse in more detail the possible effects of simplified formulations of the quantum dynamics in order to determine the most reliable scheme which can be employed with the largest possible saving of computational time.

As we briefly summarize the procedure for calculating the cross section in the framework of the CC approximation, we first need to yield the relevant T-matrix elements $T^J_{j'l'jl}(E)$ by solving the coupled differential equations from which to obtain the corresponding partial quantities $A^J_{j\to j'}$ (Gianturco 1979).

$$A^J_{j\to j'} = c_j \sum_{l,l'} |T^J_{j'l',jl}|^2 \tag{5a}$$

with

$$c_j = \frac{4\pi}{\kappa_j^2(2j+1)} \tag{5b}$$

where j, j' are the quantum numbers of the initial and final rotational states of the target. The corresponding inelastic differential cross sections are given by

$$\frac{\mathrm{d}\sigma_{j\to j'}}{\mathrm{d}\omega} = \frac{1}{(2j+1)\kappa_j^2} \sum_{m,m'} \left| \sum_{l'} (2l'+1) \left[\frac{(l'-|m-m'|)!}{(l'+|m-m'|)!} \right]^{1/2} \right.$$
$$\left. \times A_{l'}(jm \to j'm') P_{l'}^{|m-m'|}(\cos\theta) \right|^2 \tag{6}$$

in the centre of mass of the system in which the initial and final wavevectors, κ_j and $\kappa_{j'}$, are related via $\cos\theta = \vec{\kappa}_j \cdot \vec{\kappa}_{j'}$. The partial amplitudes of equation (6) are related to the averaged quantities of (5a) as

$$A^{l'}_{j\to j'} = c_j \sum_{mm'} |A_{l'}(jm \to j'm')|^2 \tag{7a}$$
$$= c_j \sum_{Jl} |T^J_{j'l',jl}|^2 \tag{7b}$$

hence

$$\sum_J A^J_{j\to j'}(2J+1) = \sum_{l'} (2l'+1) A^{l'}_{j\to j'}. \tag{7c}$$

The corresponding state-to-state integral cross sections are given by

$$\sigma_{j\to j'} = \sum_J \sigma^J_{j\to j'} = \sum_J (2J+1) A^J_{j\to j'} \tag{8a}$$
$$= \sum_{l'} \sigma^{l'}_{j\to j'} = \sum_{l'} (2l'+1) A^{l'}_{j\to j'} \tag{8b}$$

hence the partial wave contributions to the cross sections become

$$\sigma^{J(l)}_{j\to j'} = P^{J(l)}_{jj'}. \tag{8c}$$

It should be noted that the transition matrix elements $T^J_{jl,j'l'}$ are related to the scattering, S-matrix elements, the absolute square of which gives us the transition probabilities of the inelastic state-to-state processes

$$S^J_{jl\to j'l'} = \delta_{jj'}\delta_{ll'} + 2\mathrm{i}T^J_{jl,j'l'}. \tag{9}$$

Through equations (8*a*)–(8*c*) the corresponding state-to-state opacities can be given either as a function of the total angular momenta, $P^J_{jj'}(=\sigma^J_{j\to j'})$ or as a function of the final channel dynamical momentum $P^{l'}_{jj'}(=\sigma^{l'}_{j\to j'})$. Such processes are averaged over the initial orientation, m, and summed over final orientation, m', of the molecular rotor states. Because of the rapid increase in the number of j levels coupled by the potential as the collision energy increases, and because of the multiplicity effects in equations (7), the number of CC equations soon becomes very large and therefore computationally costly. One then needs to resort to more approximate dynamical treatments as often discussed in literature (for a review, see: Gianturco 1979).

The most common approximation could be introduced by removing the coupling degeneracy given by the l, l' angular momenta of the entrance and exit channels and by considering only one value of l as contributing to the sum in equation (5). Physically, this means that the collision process is seen as being dominated by short-range forces and no change of l to l' occurs in the dynamical recoupling after the scattering process. This approximation is called the centrifugally sudden, or coupled states (CS) approximation (McGuire and Kouri 1974, McGuire 1974).

One can further simplify the coupling dynamics by considering that the changes of value between the initial and final wavevectors, $|\vec{\kappa_j}|$ and $|\vec{\kappa_{j'}}|$, could be taken to be small if the amount of energy which is being transferred is much less than the relative collision energy. Thus, all channels can be considered as having the same energy and all processes are treated as occurring on the initial energy shell. This approximation is called the energy sudden (ES) approximation. When combined with the above CS scheme given rise to the more drastic infinite-order-sudden-approximation or IOS approximation (Tsien and Pack

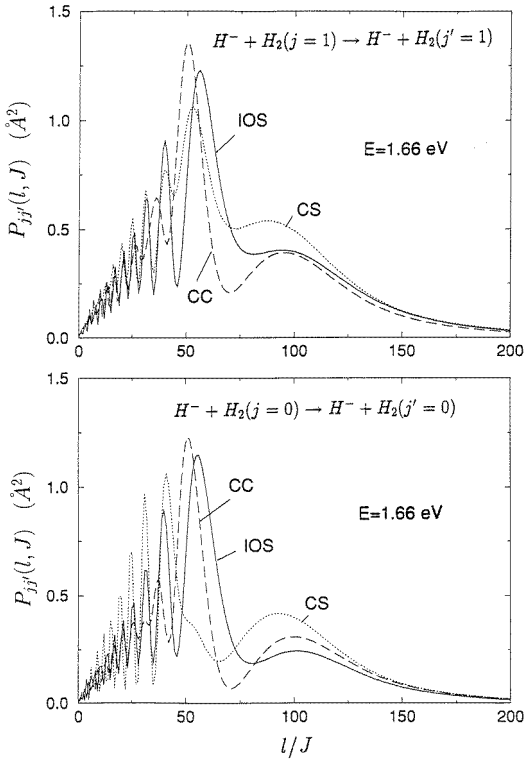

Figure 3. Comparison between the computed partial wave contributions of equation (8*c*) for the elastic processes in the IOS (full curves), CS (dotted curves) and CC (broken curves) approximations at 1.66 eV top: ortho-H_2; bottom: para H_2.

1970, Shimoni and Kouri 1977, Goldflam and Kouri 1977, Parker and Pack 1978). The latter decoupled scheme is often viewed as physically describing a scattering process during which the relative orientation of the colliding partners does not change and therefore the actual effects of anisotropic coupling are introduced only after the scattering has occurred.

Just to give an idea of the effect which such approximating schemes can have on the scattering observables, in figure 3 we present the behaviour of the computed partial functions of equations (8) for two of the state-to-state elastic processes at a collision energy of 1.66 eV, one of the energies examined in the experiments (Müller *et al* 1996). Note that, in the case of the IOS decoupling scheme, the l values coincide with the J values and therefore either index can be used to label the corresponding opacities. Thus, the quantity reported in the figure is either that of equation (8*a*) in the CS approximation or that of equation (8*b*) in the IOS approximation.

The CS calculation involved $l(J)$ values up to $l(J)_{\max} = 200$, and the number of coupled rotational states was taken up to $\Delta j_{\max} = 22$. Furthermore, the number of angles employed for the IOS quadrature (Parker and Pack 1978) was given to be 25. The results shown in figure 3 report the $P_{jj'}^{J(l)}$ (defined before) for the elastic processes at $E = 1.66$ eV. One sees that, at the collision energy of the experiments, the trajectories involving both the smaller and larger impact parameters, i.e. those sampling both the repulsive and long-range attractive regions of the interaction, behave very similarly in the two approximations and suggest that the additional ES simplification of the IOS calculations affect the opacity calculations very little. On the other hand, when the intermediate range of the intraction is being sampled by the collisions, we see that the additional energy correction of the CS scheme plays an important role and changes the size of the opacities between $30\overline{h}$ and $100\overline{h}$ values of l. This is also the region of interaction where the CC results are again different

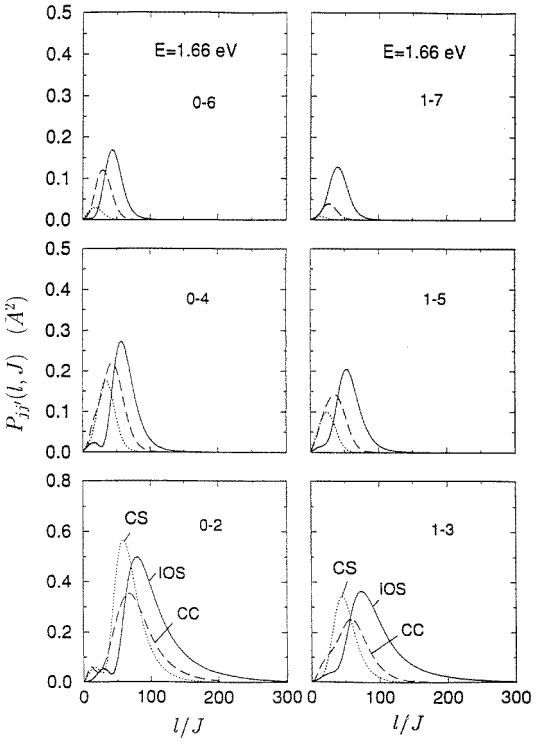

Figure 4. Comparison of the computed quantities of equation (8*c*) with different coupling schemes at fixed collision energy and for different excitation processes. Full curves: IOS results; broken curves: CC results; dotted curves: CS results.

from the previous approximations: obviously, in the interaction region where the V_λ's vary the most the correct coupling in the most reliable prescription. Thus, we expect that elastic cross sections will be different both quantitatively and qualitatively when using the CS or the IOS simplifications of the exact CC dynamics.

If we now turn to the inelastic channels, we can examine in figure 4 the behaviour of the partial cross sections for ortho-H_2 and para-H_2 targets at the same collision energy discussed before (1.66 eV). The rotationally inelastic transitions are from the initial $j = 0$ and $J = 1$ levels and we compare the corresponding opacities produced by the CC calculations (broken curves), CS calculations (dotted curves) and IOS calculations (full curves). In the case of the CC and CS calculations the number of coupled channels (or states) include four closed channels in each calculation, for a maximum of 144 coupled equations to be solved over the range of integration from the $R \approx 0$ up to $R_{\max}$= 30 a_0 (for even j values). The integrator employed was the one used in the MOLSCAT code (Hutson and Green 1993). The results of figure 4 show us the following.

(i) The IOS calculations present a larger range of $J(l)$ values which contribute to the partial opacities than in the other two coupling schemes. The differences in size become even more marked when the Δj values increase, hence the energy gaps become larger.

(ii) For the lowest two transitions ($0 \rightarrow 2$) and ($1 \rightarrow 3$), the CS calculations are closer to the CC results at large J values but differ from the CC opacities as J becomes smaller. In these excitation processes the direct coupling is dominated by the V_2 term of the interaction potential which is the main long-range coupling term. Hence, we see that both the IOS and CS calculations, because of their centrifugal decoupling scheme, fail to provide correct results at small J while the ES approximation is a good one for larger J values.

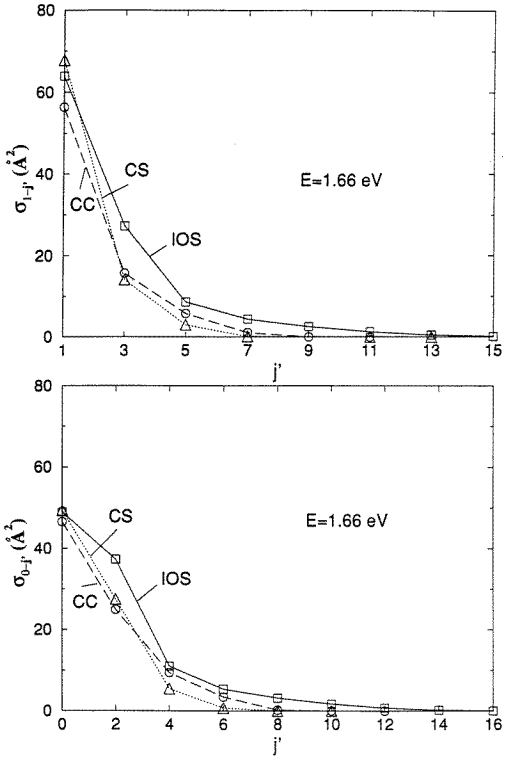

Figure 5. Computed partial integral excitation cross sections from $j = 0$ (bottom) and $j = 1$ (top) into all allowed j' values until $\Delta j = 12$. Full curves: IOS results; broken curves: CC results; dotted curves: CS results.

Table 1. Coupled states (CS) integral cross sections.

$H^- + H_2(j=0) \rightarrow H^- + H_2(j')$							
	σ (Å^2)						
E (eV)	0–0	0–2	0–4	0–6	0–8	0–10	0–12
0.1	359.94	0.19					
0.2	234.56	2.60	0.01				
0.3	177.76	6.22	0.18				
0.4	145.48	10.76	0.55	0			
0.5	122.66	14.94	1.07	0			
1.0	71.59	24.72	3.72	0.17	0	0	
1.66	50.02	27.50	5.56	0.75	0.02	0	0

$H^- + H_2(j=1) \rightarrow H^- + H_2(j')$							
	σ (Å^2)						
E (eV)	1–1	1–3	1–5	1–7	1–9	1–11	1–13
0.1	283.45	0.14					
0.2	229.38	2.69					
0.3	194.74	5.59	0				
0.4	166.22	7.84	0.06				
0.5	147.74	9.59	0.19	0			
1.0	98.93	13.01	1.50	0.02	0	0	
1.66	69.12	14.13	2.97	0.18	0	0	0

(iii) The removal of the ES approximation, when going from the IOS to the CS calculations, does not improve the agreement with the CC results for larger Δj transitions, thus indicating that the CS decoupling is still not quantitatively correct for the present system. One could note at this point that the short-range nature of the interaction mentioned earlier is sufficiently modified by its low-λ, long-range contribution to make the CS approximation an unrealistic decoupling scheme for the partial opacities related to the high-Δj excitation processes. The above results are indeed in accordance with earlier studies on the relative merits of using the IOS and CS schemes for ionic systems (see, for example Gianturco *et al* 1993)

A more specific comparison between partial inelastic and elastic, integral cross section is shown in figure 5 and tables 1 and 2. The results of the tables cover a broad range of collision energies from 0.1 to 1.66 eV and present the CS calculations up to $\Delta j = 12$ (table 1). The more exact CC calculations for the same range of transitions are shown in table 2. The values smaller than 10^{-4} are listed as zeros.

Figure 5 compares the different coupling schemes used, at a collision energy of 1.66 eV, to obtain the state-to-state integral cross sections from $\Delta j = 0$ to $\Delta j = 14$. The upper part of the figure reports transitions with odd j' values while the lower part refers to the even j' values.

The IOS cross sections, as already inferred by the behaviour of previous partial wave contributions, are always the largest ones for all transitions except for the elastic ones. On the other hand, the CC and CS results appear to be close to each other. The specific values in tables 1 and 2, however, instead show that only the $\Delta j = 2$ transitions are within 10% of each other while all the partial cross sections associated to larger Δj transitions are very different when going from the CS and CC results. The long-range part

Table 2. Close-coupling (CC) integral cross sections.

$H^- + H_2(j=0) \rightarrow H^- + H_2(j')$							
	σ (Å^2)						
E (eV)	0–0	0–2	0–4	0–6	0–8	0–10	0–12
0.1	364.37	4.27					
0.2	229.23	23.82	0.04				
0.3	162.52	38.59	0.73				
0.4	125.80	44.24	2.63	0			
0.5	102.91	44.15	5.29	0.02			
1.0	60.74	32.39	12.50	1.34	0.01	0	
1.66	46.59	24.95	9.44	3.48	0.26	0	0

$H^- + H_2(j=1) \rightarrow H^- + H_2(j')$							
	σ (Å^2)						
E (eV)	1–1	1–3	1–5	1–7	1–9	1–11	1–13
0.1	336.31	0.26					
0.2	224.49	5.52					
0.3	171.29	10.88	0.02				
0.4	139.30	14.66	0.21				
0.5	120.01	16.94	0.67	0			
1.0	77.91	18.68	4.47	0.14	0	0	
1.66	56.36	15.72	5.79	1.05	0.03	0	0

of the anisotropic interaction obviously plays an important role and the additional angular momentum recoupling which it causes between outgoing channels is not well described by the CS scheme.

This type of behaviour can be seen more pictorially by observing the elastic and inelastic cross section behaviour as a function of collision energy. It is shown by the data of figure 6, where again the ortho-H_2 transitions are presented from 0.1 to 5.0 eV. The IOS results are given by the curves with open squares. The CC calculations are labelled by open circles, while the CS results are labelled by open triangles.

The most marked effect is the difference in behaviour between elastic and inelastic cross sections. Care was taken here to ensure quantitative convergence of the elastic contributions by extending both the range of $J(l)$ values (up to $J_{max} = 200$) and the radial range of integration (up to $R_{max} = 30\ a_0$). The elastic contributions are close to each other for the CS and the CC calculations at low energies, where the IOS results differ the most, and they become similar for the higher energies examined. The IOS results, while differing at low collision energies, are also close to the latter calculations as E increases. Such effects are very much in accordance with the general behaviour of IOS, CS calculations in relation to the exact CC calculations, as often discussed by us, among others, in previous work (Gianturco and Strozhev 1994).

The inelastic contributions, on the other hand, are all very different from each other and confirm the need, for the present system, to use the correct quantum dynamics in order to obtain results with quantitative reliability. The IOS cross sections remain, as seen in figure 5, the largest partial inelastic cross section at all angles and the CC results become increasingly smaller than the latter cross sections as Δj increases. They also remain larger than the CS calculations, for which the incorrect centrifugal decoupling makes a great deal

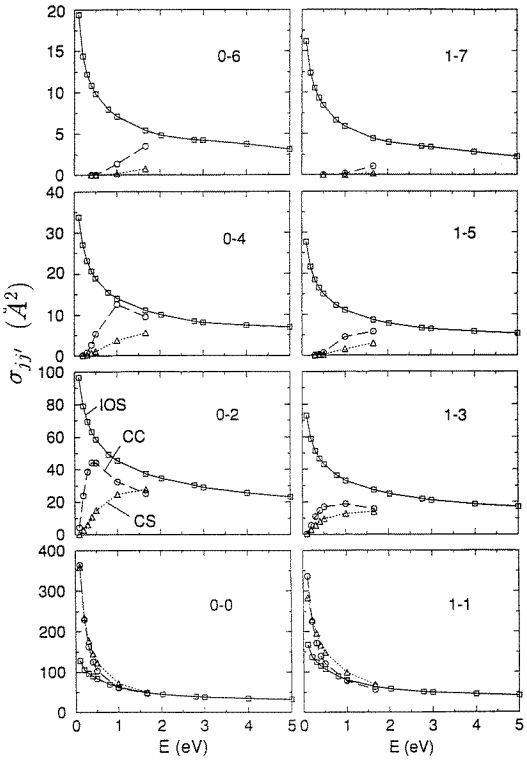

Figure 6. Computed partial integral cross sections as function of collision energy and with different coupling schemes open squares: IOS results; open circles: CC results; open triangles: CS results.

of difference.

In conclusion, we see that inelastic cross section calculations for the present system indeed require the correct angular-momentum recoupling in order to be quantitatively reliable, despite the apparent simplicity of the $H^- - H_2$ interaction anisotropy.

4. A comparison with experiments

As mentioned earlier, state-resolved measurements of rotational excitation in $H^- - H_2$ collisions at low energies have recently been published (Müller *et al* 1996) in the energy range 1.66–2.79 eV. The corresponding state-specific differential cross sections were derived from the energy-loss spectra of the scattered H^- ions and transitions ranging from $j = 1 \rightarrow 3$ to $j = 1 \rightarrow 13$ were obtained. The measurements showed the elastic scattering to be nearly absent and a strong rotational excitation of the target. Of the higher-j levels, those with $j = 5, 7, 9$ were found to be predominantly excited. At the estimated target rotational temperature $T_{\rm rot} = 180$ K of the H_2 gas beam, the experiments were considered to deal with specific populations of the rotational initial levels of n–H_2, where the $j = 0$ level was populated by 19.7%, and the $j = 1$ level by 73.7%, while the difference was given to the $j = 2$ and 3 level populations, with $j \geqslant 4$ about 0.01%.

To start to understand the quality of the rotationally inelastic processes produced by the available potential energy surface (Stärck and Meyer 1993) in figure 7 we present the behaviour of the lower rotationally inelastic transitions at the collision energy of 1.66 eV. In the upper part of the figure we report the experimental points for the $j = 1 \rightarrow j' = 5$ excitation (open circles) and show for them the experimentally stated error bars on their

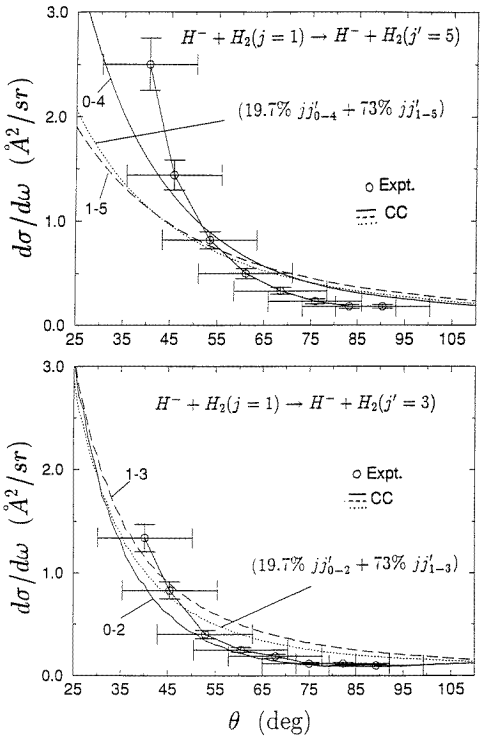

Figure 7. Comparison between computed and measured differential cross sections (DCS) at a collision energy of 1.66 eV. The DCS are in $Å^2$/sr and θ is the centre-of-mass angle. Experimental points (from Müller *et al* 1996): open circles. Broken, dotted and full curves: CC calculations, Top: $\Delta j = 4$ for ortho H_2; bottom $\Delta j = 2$ for ortho H_2.

size and angular resolution. The corresponding energy loss of H^- had an estimated energy resolution of about 50 meV; hence, we see that the energetics of the $j = 0 \rightarrow j' = 4$ excitation (150.8 meV) and that of the $j = 1 \rightarrow j' = 5$ excitation (211.1 meV) could only be revealed as a single process in the experimental observation. Correspondingly, the experimental observation of the $j = 1 \rightarrow j' = 3$ process (75.4 meV) and of the $j = 0 \rightarrow j' = 2$ excitation (45.2 meV) could also appear as contributing to the same energy-loss peak of the H^- projectile. The analysis of the experimental data, and their comparison with our present calculations, therefore must take the above points into consideration as indicated in figure 7.

The top part of figure 7 shows, in fact, the excitation angular distributions, at 1.66 eV, for the observed $j = 1 \rightarrow j' = 5$ process. The relevant calculations are therefore the $(0 \rightarrow 4)$ and $(1 \rightarrow 5)$ excitation cross sections and their CC values are shown, respectively, by the full and broken curves. In the bottom part of figure 7 we show the excitation process associated to the $(1 \rightarrow 3)$ transition. The experimental values are given by the open circles and are marked by the error bars in the angular and intensity resolutions. The corresponding calculations refer to the $(0 \rightarrow 2)$ and $(1 \rightarrow 3)$ transitions, given by the full and broken curves respectively.

It is also interesting to note that, when one takes into consideration the relative populations of the initial levels in the beam ($j = 0$ and 2) the results are given, for the two excitation processes described in that figure, by the dotted curves reported at the top and the bottom and compared with the experimental data.

This comparison clearly shows that the lower excitation processs with $\Delta j = 2$ which is mostly driven, as discussed before, by the $\lambda = 2$ direct coupling potential, appears to be given by the present calculations in rather good accord with experiments, both in magnitude

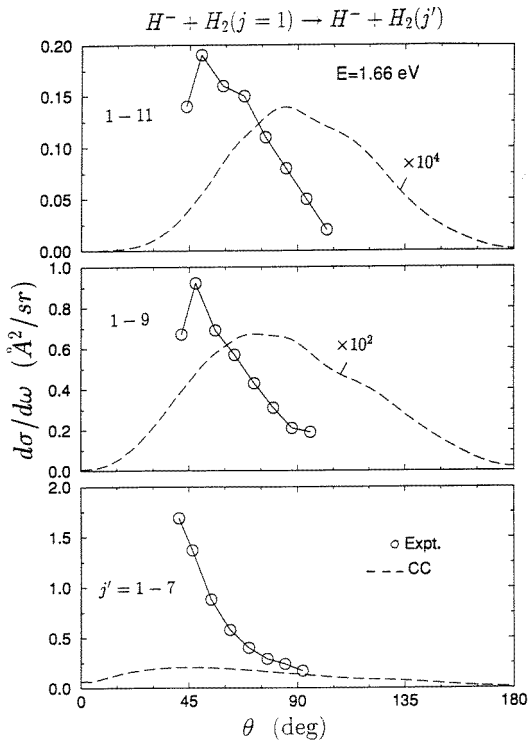

Figure 8. Comparison between experimental and computed DCS for inelastic processes with ortho H_2 at 1.66 eV. Open circles: experiments from Müller *et al* (1996). Broken curves: CC calculations.

and in angular distribution. On the other hand, the next-higher excitation cross section indicates smaller values than those given by experiments in the forward scattering region of the small θ values, with the latter being the centre-of-mass scattering angle. Thus, although the agreement with theory is also rather satisfactory for this excitation process, in the angular range beyond $\theta \approx 40^\circ$, we begin to see that the long-range part of the interaction is possibly yielding anisotropic couplings which are not strong enough to reproduce the experiments.

Such a trend is seen even more markedly in the comparison between computed and measured angular distributions for the excitation processes associated with larger Δj transitions and presented in figure 8. The energy value chosen is the same as before, i.e. 1.66 eV, and the transitions reported are for $\Delta j = 6, 8$ and 10 in going from the bottom to the top of the figure. We have shown the ortho-H_2 transitions because the experimental data for them are considered to be more quantitatively reliable than those related to the para-H_2 transitions (Müller *et al* 1996).

The comparison clearly shows that the computed behaviour of the state-to-state angular distributions is very much at variance, in terms of magnitude, with that given by the deconvolution of the experiments (open circles in the figure). The differences also increase as the Δj values increase and reach various orders of magnitude for the transitions associated with the largest Δj values. It is difficult here to reliably assess the confidence level of the experimental deconvolution in order to attach more quantitative error bars to the final state-to-state cross sections (Müller *et al* 1996). On the other hand, it is unlikely to assume that the experimental data are too big by orders of magnitude. In this case, therefore we can only conclude that the computed anisotropy of the $H^- - H_2$ interaction for the higher contributions to the multipolar expansion of equation (4) is too weak especially in its long-range region. This is the region that would affect the forward scattering behaviour the most

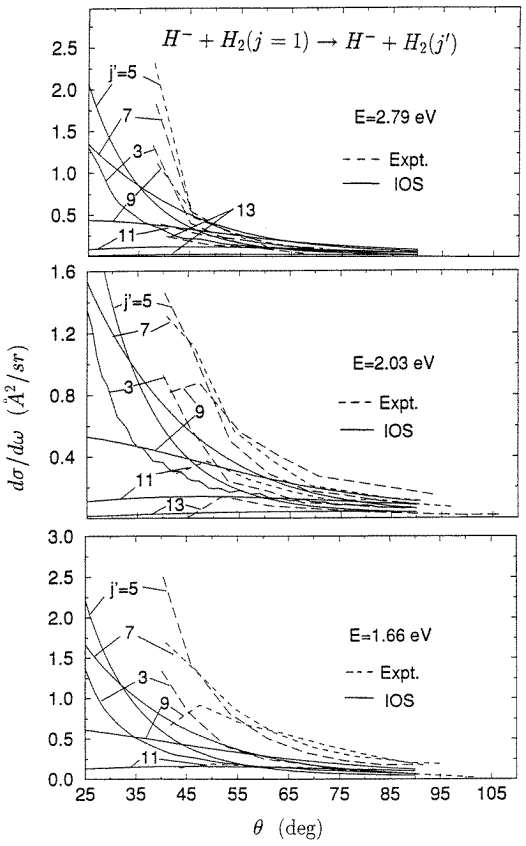

Figure 9. Partial inelastic DCS for rotational excitation of ortho-H_2 at three different collision energies. Broken curves: experiments from Müller *et al* (1996); full curves: present IOS calculations.

out of the computed inelastic cross sections.

In order to further analyse this point at higher collision energies, where scattering trajectories should sample with increasing importance the shorter-range region of the interaction, we show in figure 9 the behaviour of the angular distribution for the state-to-state excitation processes measured at 2.03 and 2.79 eV. Since the CC calculations would be far too expensive as E increases, we decided to make the comparision with the more approximate IOS calculations. The general *caveat* here should be that our previous analysis of the various coupling schemes showed the IOS excitations to be always larger than the CC and CS results. Thus, we should take these computed quantities to be the upper bounds to the results from more accurate calculations with the same interaction potential. For a comparison with the previous results at 1.66 eV we show the IOS calculations, at that same energy, at the bottom of figure 9.

The IOS calculations at all the three energies of that figure indicate an angular dependence which qualitatively follows the experimental data. Furthermore, the inelastic processes are now given by our computations to be of the same order of magnitude as their experimental counterpart, a feature obviously related to the larger size of the IOS inelastic cross sections. Finally, we see that, as the collision energy increases, the computed and measured quantities agree very closely in the large θ regions while differ very markedly in the forward scattering regions. In other words, we see, even with the large cross sections given by IOS calculations, that the experimental data still appear to yield excitation probabilities in the forward direction, that are larger than the computed ones, where the

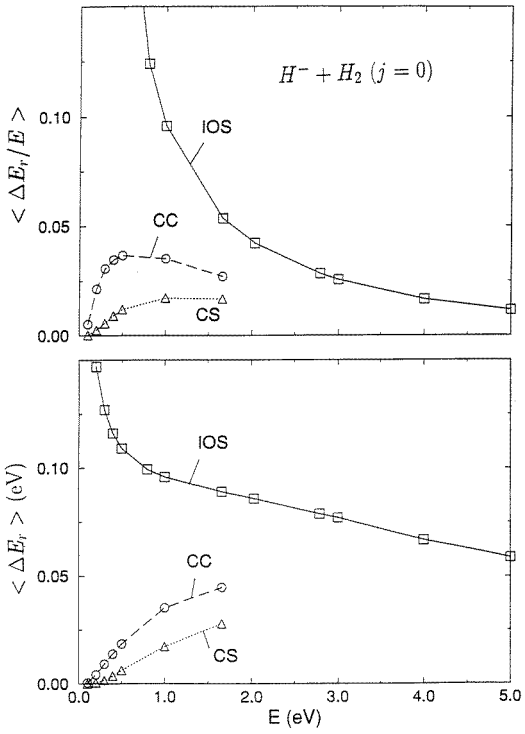

Figure 10. Computed average energy transfer values as function of collision energy for para-H_2 at $j = 0$. Open squares: IOS calculations; open circles: CC calculations; open triangles: CS calculations.

long-range anisotropy of the interaction plays its greatest role.

The final quantity shown in figure 10 now refers to one of the common indicators of rotational excitation efficiency in low-energy scattering processes. This is the average rotational energy transfer given, the para-H_2 in its $j = 0$ initial level as

$$\langle \Delta E_r \rangle = \frac{\sum_{j'} \sigma(j = 0 \rightarrow j') \Delta E_{jj'}}{\sum_{j'} \sigma(j = 0 \rightarrow j')}. \tag{10}$$

Or the scaled relative quantity $\langle \Delta E_r / E \rangle$ which also includes the collision energy value.

We see that the latter indicator, shown in the top part of figure 10, clearly distinguishes between the IOS results and the CC, CS calculations which yield invariably smaller values. They suggest that, for collision energies up to 1.66 eV the amount of energy which is being transferred to rotations is no more than 2–3%, clearly at variance with the experimental indications (Müller *et al* 1996). Furthermore, the actual average values are shown to be up to about 100 meV of energy into rotation from the IOS results, which are thus not far from the experimental indications. On the other hand, the CC, CS results never rise above 50 meV.

5. Summary and conclusions

The present calculations have analysed in some detail the relative size and angular behaviour of the rotationally inelastic processes which have recently been measured in $H^- - H_2$ scattering experiments (Müller *et al* 1996). Using a previously computed PES (Stärck and Meyer 1993) we found that the lower excitation processes from $j = 0$ and $j = 1$ initial levels into $j' = 2$ and 4, or $J' = 3$ and 5, are produced by the theoretical treatment in rather good

agreement with the corresponding experimental quantities. Furthermore, the comparison between different coupling schemes for the quantum treatment of the rotationally inelastic scattering shows that this system, despite its apparent simplicity, requires a rather careful handling of the angular-momentum recoupling in the outgoing channels, hence, it is not quantitatively described by the CS and IOS decoupled approximation.

The analysis of the excitation processes corresponding to larger Δj transitions and up to $\Delta j = 12$, on the other hand, has shown here that the computed values are at the variance with their experimental counterpart and generally come out from the calculations to be much smaller than the measured values, this being more so when Δj increases. The corresponding evaluation of the efficiency of energy-transfer collisions into rotational levels also suggests that the presently employed PES is possibly too weakly anisotropic in its long-range part. Just to give an example, the total integral cross sections estimated from experiments suggest a value for the total excitation from $j = 1$ to be between 20–30 Å^2 (Müller *et al* 1996) at a collision energy of 1.66 eV, while the present calculations find σ_{rot} at the same energy to be given by CC calculations as 22.59 Å^2 (table 2), i.e. slightly smaller than the value proposed by the experiments.

On the other hand, this is a further example for H^- dynamics in which the experimental findings are directly compared with rigorous calculations at the quantum, *ab initio* level and therefore expect to gain from it even further insight on the interplay between potential features and dynamical attributes from low-energy collisions.

Finally, one should keep in mind that the vibrationally inelastic processes are not considered neither in the present calculations nor are they extracted from the experimental data. However, our study of the vibrational coupling and its comparison with other experiments (Gianturco and Kumar 1995b, c) indicates that these processes carry very little probability, while the channels indicated by equations (1) and (2) cannot be excluded with certainty.

Acknowledgments

Several clarifying discussions with Professor F Linder on his experimental data are gratefully acknowledged. We also thank the Max–Planck Society for the financial support of SK during his stay in Rome. Computational facilities and support were provided by the Supercomputer Center in Rome (CASPUR), the Italian National Research Council (CNR) and the Italian Ministry for University and Research (MURST). We are also grateful to one of the referees for carefully reading our manuscript.

References

Boothroyd A I, Keogh W J, Martin P G and Peterson M R 1996 *J. Chem. Phys.* **104** 7139–52
Choi B H and Tang K T 1975 *J. Chem. Phys.* **63** 1783–96
Flower D R and Wroe R A 1996 *J. Phys. B: At. Mol. Opt. Phys.* **29** L851–4
Gianturco F A 1979 *The Transfer of Molecular Energies by Collisions* (Berlin: Springer)
Gianturco F A and Kumar S 1995a *Chem. Phys.* **196** 485–97
——1995b *J. Phys. Chem.* **99** 15 342–7
——1995c *J. Chem. Phys.* **103** 2940–8
——1996 *Z. Phys.* D **37** 155–64
Gianturco F A, Kumar S and Schenider F 1996 *J. Chem. Phys.* **105** 156–64
Gianturco F A, Serna S, Palma A, Billing G D and Zenevich V 1993 *J. Phys. B: At. Mol. Opt. Phys.* **26** 1839–49
Gianturco F A and Strozhev A 1994 *J. Chem. Phys.* **101** 9624–34
Goldflam R and Kouri D J 1977 *J. Chem. Phys.* **67** 5661–78

Hege U and Linder F 1985 *Z. Phys.* **320** 95–104
Hutson J M and Green S 1993 *MOLSCAT Computer Code Version 14, Distributed by the CC Project no 6 (CCP6) of the EPSRC, UK*
McGuire P 1974 *Chem. Phys.* **4** 483–98
McGuire P and Kouri D J 1974 *J. Chem. Phys.* **60** 2488–501
Mahapatra S and Sathymurty N 1996 *J. Phys. Chem.* **100** 2759–61
Mahapatra S, Sathyamurty N, Kumar S and Gianturco F A 1995 *Chem. Phys. Lett.* **24** 223–8
Metz R B, Bradforth S E and Neumark 1992 *Adv. Chem. Phys.* **8** 1–34
Müller H, Zimmer M and Linder F 1996 *J. Phys. B: At. Mol. Opt. Phys.* **29** 4165–78
Niedner-Schatterburg G and Toennies J P 1992 *Adv. Chem. Phys.* **82** 553–97
Parker R and Pack R T 1978 *J. Chem. Phys.* **6** 1585–99
Reinig P, Zimmer M and Linder F 1992 *Nucl. Fusion A M Suppl.* **2** 95–107
Shimoni Y and Kouri D J 1977 *J. Chem. Phys.* **66** 2841–56
Stärck J and Meyer W 1993 *Chem. Phys.* **176** 83–95
Sun Y and Dalgarno A 1994 *Astrophys. J.* **427** 1053–67
Truhlar D G and Herowitz C J 1978 *J. Chem. Phys.* **68** 2466–84
Tsien T P and Pack R T 1970 *Chem. Phys. Lett.* **6** 54–6
Zimmer M and Linder F 1992 *Chem. Phys Lett.* **195** 153–8